# SUPPLEMENTARY MATERIALS

# Generic strategy for the synthesis of highly specific Au/MIP nanozymes and their application in homogeneous assays

Shaemaa Hadi Abdulsada,[1,2] Alvaro Garcia Cruz*[1], Christopher Zaleski, [1] Elena Piletska, [1] Damla Ulker,[1] Stanislav Piletsky[3], Sergey A. Piletsky[1]

[1]University of Leicester, Chemistry Department, University Rd, Leicester LE1 7RH, United Kingdom

[2]Mustansiriyah University, College of Science, Chemistry Department, 10047, Baghdad, Iraq.

[3]Memorial Sloan Kettering Cancer Center, 1275 York Avenue, ZRC-13S, New York, NY 10065, USA

## 1. Materials

All reagents were available and used directly without further purification. Sodium hydroxide (NaOH), phosphate-buffered saline (PBS) (Sigma-Aldrich, Gillingham, UK), glass beads of 9–13 μm in diameter provided by Sigma Aldrich. Anhydrous toluene, (3-iodopropyl)trimethoxysilane, borate buffer, phosphate buffer, carbonate buffer, amphetamine, mercaptoethanol, 2,2′-(ethylenedioxy)bis(ethylamine), dansyl chloride, acetonitrile, acrylic acid (AAc), N-3-Aminopropyl meth acrylamide (APM), N-isopropyl acrylamide (NIPAm), N-tert-butyl acrylamide (TBAm), N,N'-methylenebisacrylamide (MBAA), gold stock solution, hydrogen peroxide 50%, acetone, ethanol, bromopyrogallol dye and amphetamine were acquired from Merk. ). For the elution and purification of Nanozymes, solid phase extraction tubes (SPE) with polyethylene frit (20 μm porosity, Supelco), disposable plastic syringes with cellulose acetate syringe filter (25 mm, 0.45 μm, Whatman) and a SnakeSkin dialysis tubing (10K MWCO, 22 mm diameter, 11 cm Tubing Length, 3.3 mL cm-1 Thermo Scientific) were used.

## 2. Characterization of nanoparticles

The infrared spectroscopy analysis was performed using a Bruker Alpha platinum-ATR FTIR spectrometer. The Nanozyme spectrum indicates the presence of amide band, and characteristic polyacrylamide peaks (R-NH-CO-R), such as those of N-H stretching and asymmetric vibration (3300-3600 $cm^{-1}$) and N-H bending (600 $cm^{-1}$). Also, C=O (1500–1650 $cm^{-1}$), and –C-N stretching vibration (1400 $cm^{-1}$) were observed. The signals at < 1500 $cm^{-1}$ indicates carbonyl group connected to carbon chain while vibrations at 1250–1350 $cm^{-1}$ indicates C-H asymmetric vibrations. [1] Also, C-C vibration (1160 $cm^{-1}$) was observed as shown in **Figure S1**. Given the intricate nature of the amide-based molecularly imprinted polymer, we can anticipate a discernible presence of acrylic acid primarily in the spectral range around 1700 $cm^{-1}$.[2] It's worth noting that this specific region is where the MIP and NIP signals diverge, as illustrated in the Figure 1 insert below. Remarkably, in this region, the NIP signal exhibits greater intensity than the MIP signal, suggesting a higher proportion of acrylic acid integrated into the structure of the NIP. This is possibly due to the effect of the template during the solid phase synthesis.

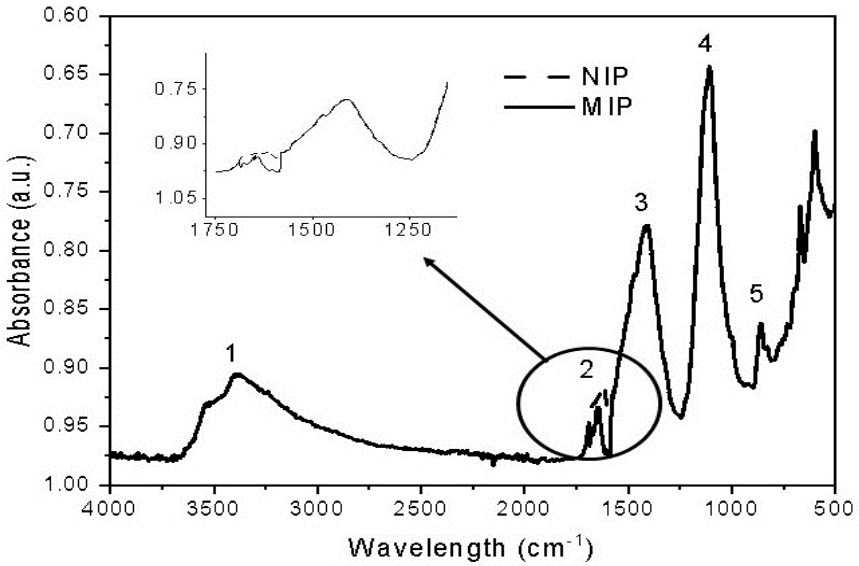


**Figure S1**. FTIR spectra overlapped for (a) Nanozyme nanoparticles and (b) control NIP. The spectra show characteristic sigla for (1) Amide bands, (2) Carbonyl group, (3) Amide peaks, (4) and (5) Hydrogen carbon vibrations.

## 3. Preparation of glass beads

Firstly, 60g of glass beads were activated by boiling in 30 mL NaOH 1 M for 15 min and then washed with distilled water (100 mL × 10 times) and 5 mM PBS (2 × 100 mL), respectively. Afterwards, glass beads were washed with acetone (100 mL × 4 times) and dried under vacuum until fully dry. Subsequently, glass beads were silanized by incubation in 4% (3-iodopropyl) trimethoxysilane (1 mL) in 25 mL dry toluene for 8h. The glass beads were then washed with dry acetone (100 mL × 2 times) and dried under vacuum. To confirm the functionalization, adaptation of the Dansyl chloride test for primary amines was performed. To some extent, the method was modified as follows: 1 g of salinized glass beads were incubated for 1 h in 5 mL of 1 mM 2, 2′-(ethylenedioxy) bis (ethylamine) in DMF. Afterwards, the glass beads were washed (5 mL × 3 times) with DMF. Subsequently, the glass beads were incubated in 5 mL (1mg $mL^{-1}$) dansyl chloride in DMF and incubated for 1 h in the dark. After that, the glass beads were washed with DMF (10 mL × 2 times) and fluorescence was observed under the UV lamp at 340/540 nm (excitation/emission). The same procedure was repeated with non-silanized glass beads. The silanized glass beads were fluorescent, while the non-silanized glass beads were non-fluorescent under the UV lamp, which confirmed the successful salinization of the glass beads.

## 4. Assay principles.

Dynamic light scattering (DLS) measurements were performed using a Zetasizer Nano (Nano-S) from Richmond Scientific Instruments Ltd. (Lancashire, UK). For these measurements, 1 mL solution of nanoparticles was ultra-sonicated for 3 min, to disrupt potential agglomerates. Each sample runs 6 times. (PDI) polydispersity index and particle size as hydrodynamic diameter were measured. The polydispersity index indicates the "accuracy of the measurement in a mono-disperse sample with acceptable values between 0 and 0.7".

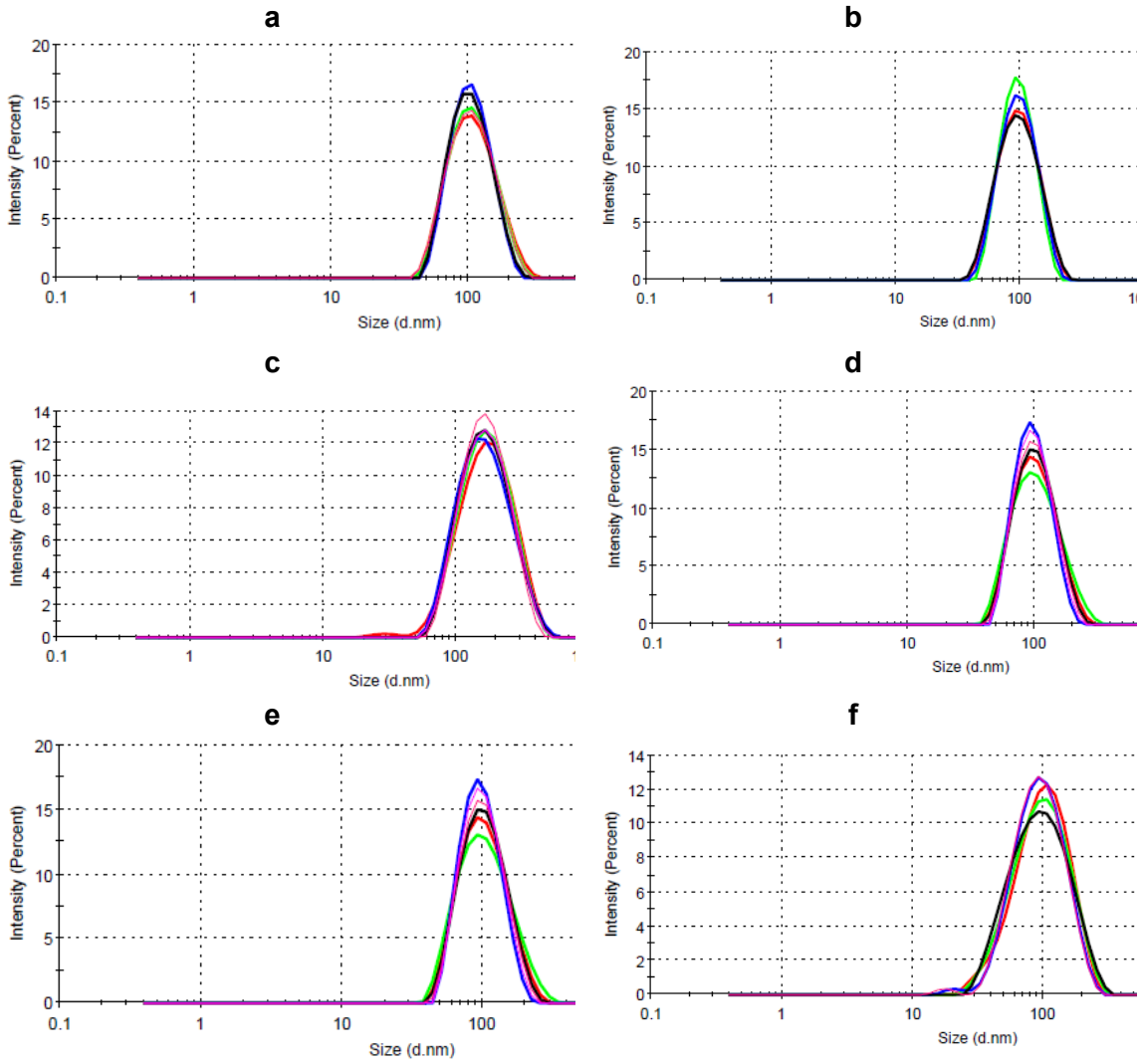


| Particle | Size | Change in Size |
|---|---|---|
| (a) Nanozyme in water. | 98.4 ± 1.5 nm (PDI = 0.13) | - |
| (b) NIP in water | 89.01 ± 3.1 nm (PDI = 0.12) | - |
| (c) Nanozyme after Amphetamine | 149.0 ± 8.3 nm (PDI = 0.18) | 51.4% |
| (d) NIP after Amphetamine | 91.35 ± 7.8 nm (PDI =0.15) | 2.6% |
| (e) Nanozyme after Paracetamol | 102.7 ± 2.6 nm (PDI = 0.23) | 4.4% |
| (f) NIP after Paracetamol | 90.21 ± 5.1 nm (PDI =0.17) | 1.3% |

**Figure S2**: DLS of (a) Nanozyme and (b) NIP in water. Hydrodynamic size after injecting of Amphetamine (20 µl ,100 nM) for (c) Nanozyme and (d) NIP. Hydrodynamic size after injection of Paracetamol (20 µl ,100 nM) for (e) Nanozyme and (f) NIP. The volume analysed of Au/MIP and Au/NIP was 300 µL at 0.5 mg $mL^{-1}$.

Generally the Fenton reaction describes the generation of hydroxyl radicals ($HO^{\bullet}$) through the activation (reduction) of hydrogen peroxide ($H_2O_2$) by ferrous ($Fe^{2+}$) ions as as shown in **Scheme S1** (I-III).[3] Due to the potential of the Fenton and Fenton-like reactions in generating highly reactive hydroxyl radicals, it has also been employed extensively as an initiation system for free radical polymerization.[4] Polymerization of alkenes by $H_2O_2$ activation by Fenton and Fenton-like reactions proceeds via multiple reactions as described in **Scheme S1** (I-V).[5] Fenton catalysts generate hydroxyl radicals ($HO^{\bullet}$) which abstract hydrogen atom from organic molecules to form a radical monomer, which subsequently undergoes redox coupling and polymerization reactions. In the presence of excess $H_2O_2$ and monomer the rate of polymerization is ultra-fast, and the oxygen evolution from $H_2O_2$ is suppressed.

$$Fe^{2+} + H_2O_2 \rightarrow Fe^{3+} + HO^{\bullet} + OH^{-} \quad (I)$$

$$Fe^{3+} + H_2O_2 \rightarrow Fe^{2+} + HO_2^{\bullet} + H^{+} \quad (II)$$

$$Fe^{2+} + HO^{\bullet} \rightarrow Fe^{3+} + OH^{-} \quad (III)$$

$$HO^{\bullet} + CH_2{=}CHR \rightarrow HOCH_2\text{-}C^{\bullet}HR \quad (IV)$$

$$HOCH_2\text{-}C^{\bullet}HR + CH_2{=}CHR \rightarrow HOCH_2\text{-}CHR\text{-}CH_2\text{-}C^{\bullet}HR \quad (V)$$

**Scheme S1.** The Fenton reaction generates hydroxyl radicals (HO•) by activating hydrogen peroxide ($H_2O_2$) with ferrous ions ($Fe^{2+}$), depicted in steps (I-III). Fenton-like reactions initiate highly reactive hydroxyl radicals for free radical polymerization in steps (IV-V).

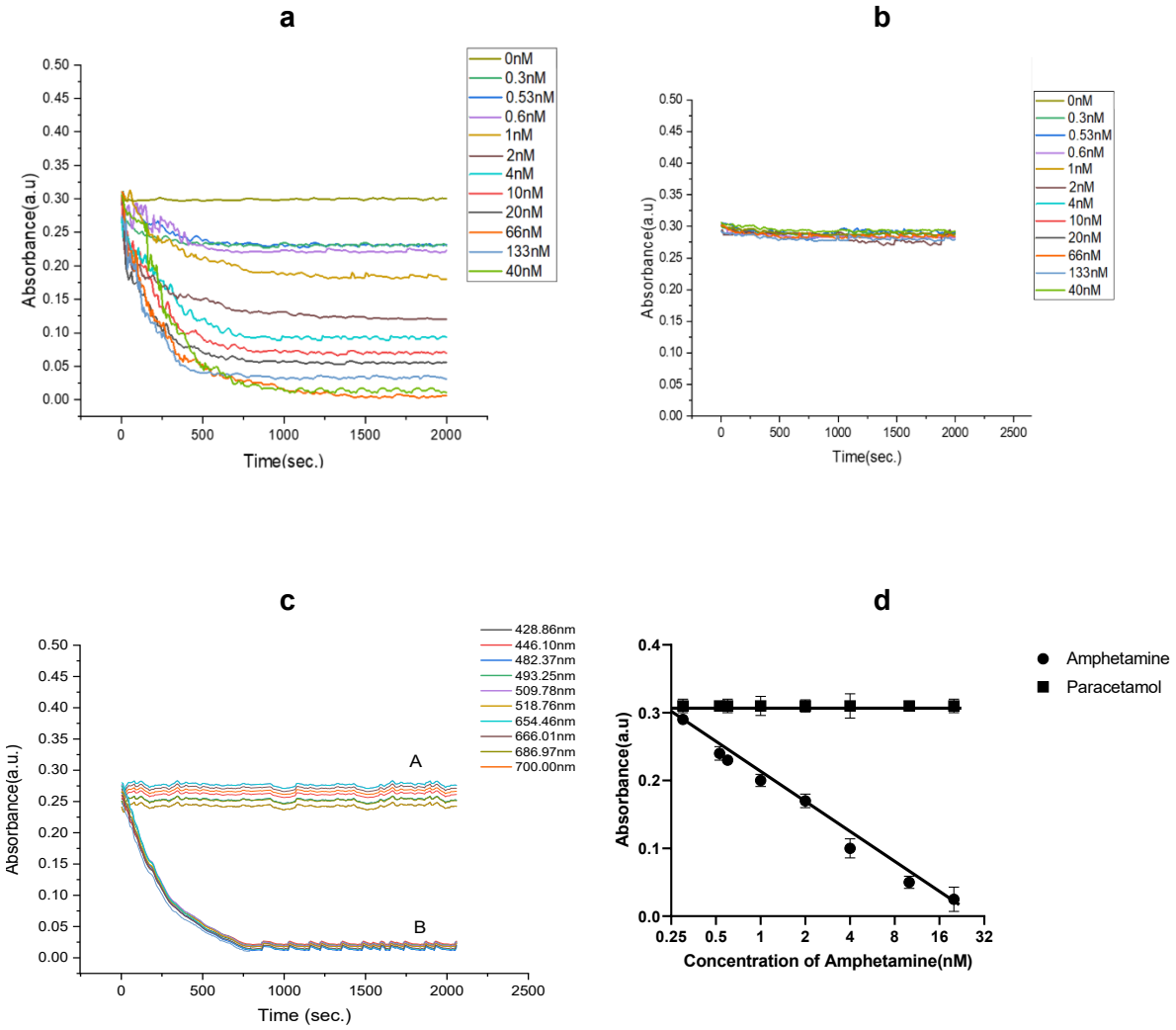


**Figure S3**: LSPR response of AuMIP-1 to different (a) Amphetamine, and (b) Paracetamol concentrations (0, 0.3, 0.53, 0.6, 1, 2, 4, 10, 20, 40, 66.7, and 133.3 nM). Continuous flow injection experiments performed using 2 mL of AuMIP1 (0.5mg/mL) and analyte rate flow at 10 µl/min and recorded for 2000 s. (c) LSPR response of AuMIP-1 to (A) 500 nM Paracetamol and (B) 500 nM Amphetamine. (d) Corresponding calibration plot for the LSPR response of AuMIP-1 to different amphetamine and paracetamol at the linear range (0.3 to 20 nM).

## 5. Assay optimization.

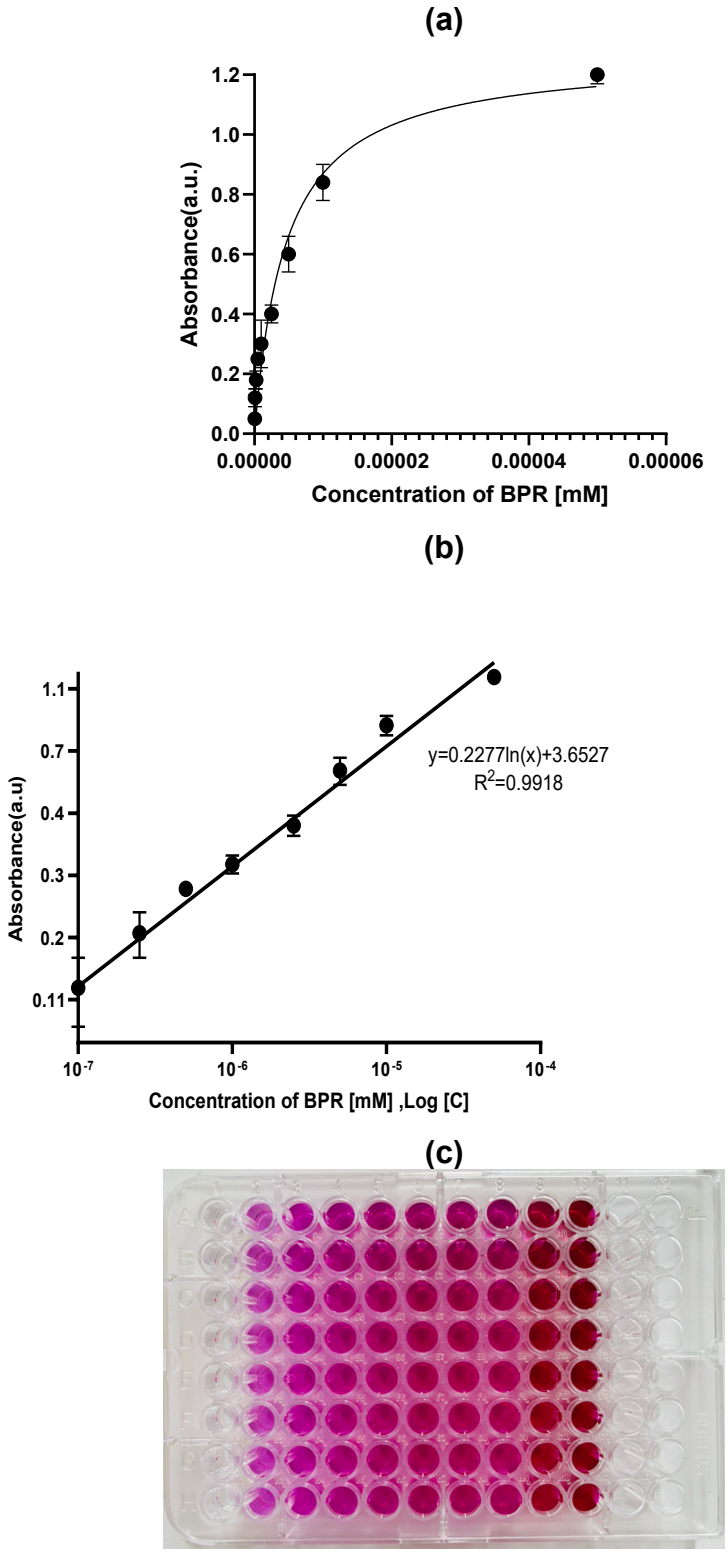


**Figure S4**. Calibration plot for BPR in 5 mM PBS buffer pH 7, (a) BPR concentration against absorbance and (b) the respective logarithmic plot at different BPR concentrations (0.0 nM, 0.005 nM,0.001 nM,0.025 nM, 0.05 nM , 0.1 nM 0.25nM,0.5 nM ,1 nM, and 5nM). (c) colour obtained in the 96 well microplate employed.

To optimise pH, calibration plots of BPR were built at different pH levels from pH 6,0 to pH 9,0, as depicted in **Figure S5** and detailed in **Table S2**. The pH was found to impact the ionization state of BPR, consequently affecting the availability of protons and other chemicals involved in the oxidation process on the gold surface. Additionally, the Au/MIP nanozymes demonstrated a tendency to aggregate at elevated pH levels, resulting in a loss of its activity. Consequently, all following experiments were performed at pH 7,0.

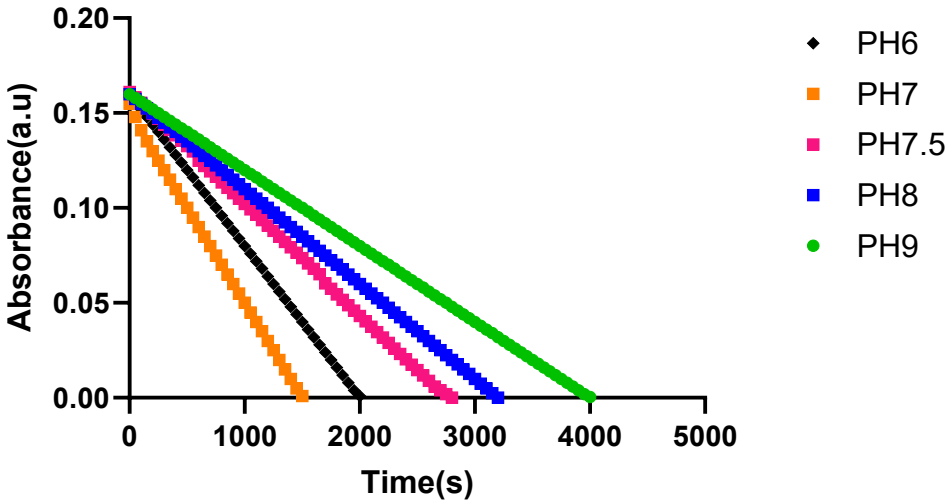


**Figure S5.** The effect of pH on the Nanozyme assay was optimized using kinetic mode and measuring the change in absorbance of BPR against time. For the pH optimization, 5 mM PBS was employed (pH 6-8), while carbonate buffer was used for pH 9. Each well contained 10 µL of the Nanozyme (0.4 mg×mL$^{-1}$), 135 µL of 10 nM BPR prepared with buffer at pH (6, 7, 7.5, 8 and 9), 135 µL of $H_2O_2$ 50% and 20 µL of 40 nM amphetamine.

**Table S2.** The effect pH levels on the Nanozyme assay**.**

| pH level | Slope (a.u.×s$^{-1}$) | Slope (nM×s$^{-1}$) | Linearity ($R^2$) |
|---|---|---|---|
| 6 | -6.02×10$^{-5}$ | -6.02×10$^{-5}$ | 0.920 |
| *7* | *-1.02×10$^{-4}$* | *-1.02×10$^{-4}$* | *0.999* |
| 7.5 | -5.85×10$^{-5}$ | -5.85×10$^{-5}$ | 0.999 |
| 8 | -5.00×10$^{-5}$ | -5.00×10$^{-5}$ | 0.999 |
| 9 | -4.00×10$^{-5}$ | -4.00×10$^{-5}$ | 0.999 |

The BPR reaction rate was compared for different Au/MIP nanozyme concentrations, as illustrated in **Figure S6** and detailed in **Table S3**. As the Au/MIP nanozymes concentration increased from 0.2 to 0.4 mg×mL$^{-1}$, the catalytic activity increased.

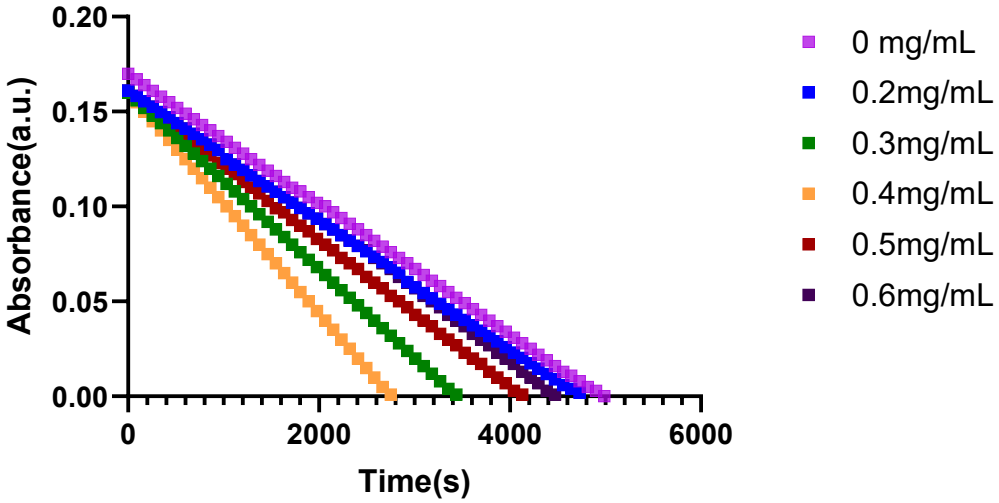


**Figure S6**. The effect of the Nanozyme concentration on the assay optimized using kinetic mode and measuring the change in the BPR absorbance at pH 7 in 10mM PBS: Each well contained 10 µL of the Nanozyme (0, 0.2, 0.3, 0.4, 0.5 and 0.6 mg×mL$^{-1}$), 135 µL of 10 nM BPR prepared with buffer at pH (6, 7, 7.5, 8 and 9), 135 µL of $H_2O_2$ 50% and 20 µL of 40 nM amphetamine.

**Table S3.** The effect of different Nanozyme concentrations on the assay

| MIP [mg mL$^{-1}$] | Slope (a.u.×s$^{-1}$) | Slope (nM×s$^{-1}$) | Linearity ($R^2$) |
|---|---|---|---|
| 0 | -3.42×10$^{-5}$ | -3.42×10$^{-5}$ | 0.999 |
| 0.2 | -3.41×10$^{-4}$ | -3.41×10$^{-4}$ | 0.999 |
| 0.3 | -4.65×10$^{-5}$ | -4.65×10$^{-5}$ | 0.999 |
| *0.4* | *-5.81×10$^{-5}$* | *-5.81×10$^{-5}$* | *0.999* |
| 0.5 | -3.87×10$^{-5}$ | -3.87×10$^{-5}$ | 0.999 |
| 0.6 | -3.59×10$^{-5}$ | -3.59×10$^{-5}$ | 0.999 |

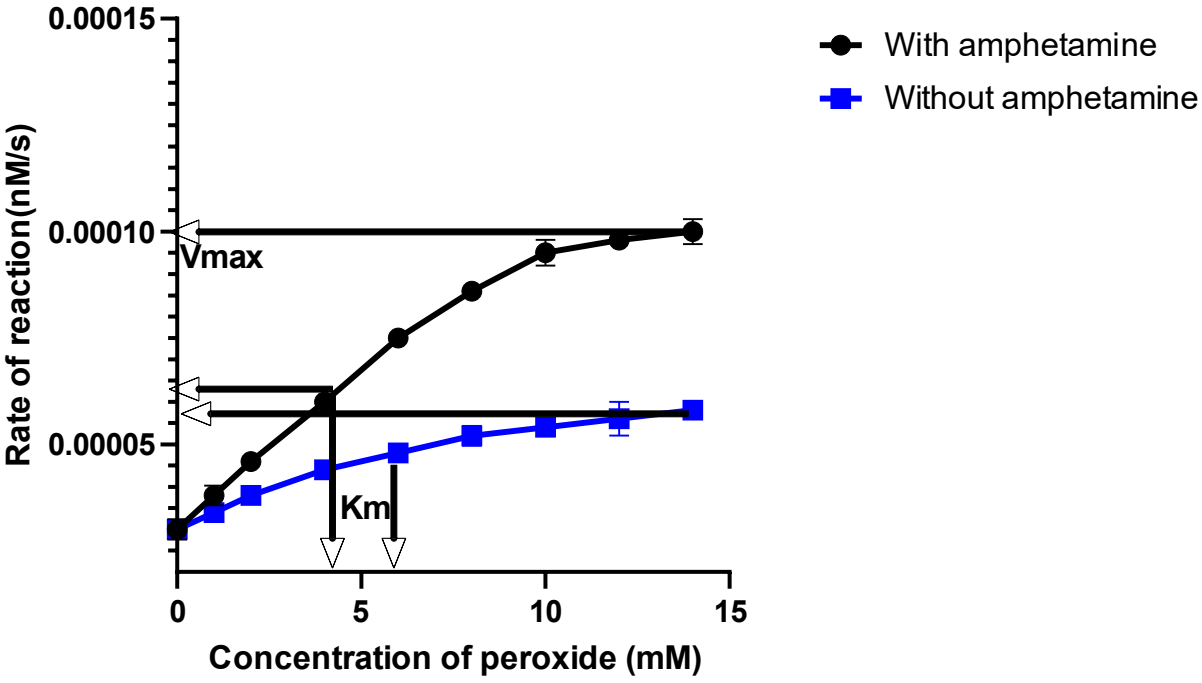


**Figure S7**. The relationship between various peroxide concentrations and the reaction rate is used to calculate Km. Each well contained 10 µL of the Nanozyme (0.4 mg×mL$^{-1}$), 135 µL of 10 nM BPR at pH 7 in 5 mM PBS, 20 µL of amphetamine (40 nM) and 135 µL of $H_2O_2$ in the concentration range of (0.0, 1.0, 2.0 ,4.0 ,6.0 ,8.0 ,10.0 ,12.0 and 14.7 mM).

.

**Table S4**. Michaelis-Menten constant (Km) and Vmax in assay

| Condition | Km (mM) | Vmax (a.u/sec.) | Vmax (nM×s$^{-1}$) |
|---|---|---|---|
| *With Target* | *4.0* | *1.0×10$^{-4}$* | *1.0×10$^{-4}$* |
| Without target | 6.0 | 5.8×10$^{-5}$ | 5.8×10$^{-5}$ |

To establish the working range, the assay's response was measured at varying concentrations of amphetamine (0.3-133.3 nM), as depicted in **Figure S8** and detailed in **Table S5**. The highest reaction rate was achieved at 66.7 nM, and no significant differences were observed beyond this concentration, as demonstrated in **Figure 3**. One plausible explanation for this phenomenon is that, beyond this concentration, Nanozyme actuation becomes inactivated due to saturation.

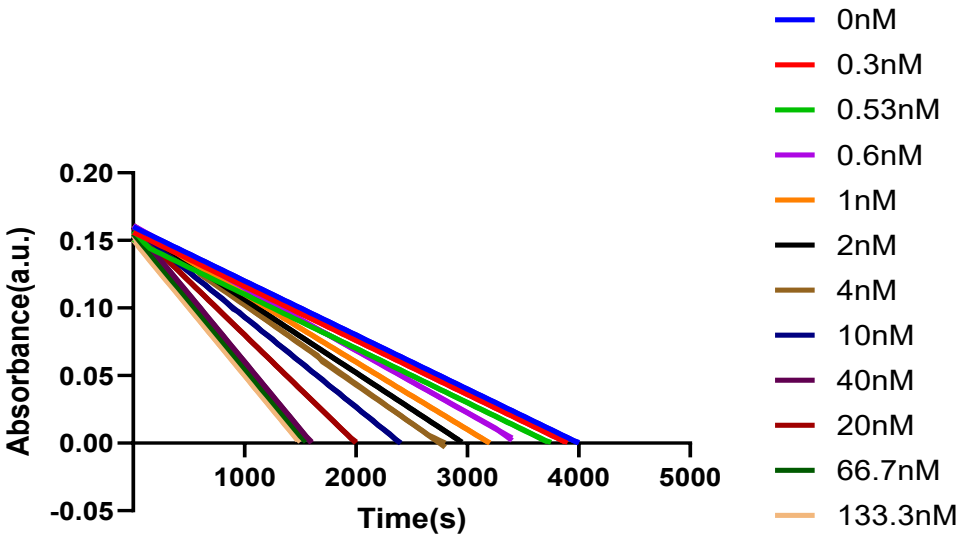


**Figure S8**. Study of amphetamine working linear range in the nanozyme assay. Each well contained 10 µL of the Nanozyme (0.4 mg×mL$^{-1}$), 135 µL of 10 nM BPR at pH 7 in 5 mM PBS, 135 µL of $H_2O_2$ 50% and 20 µL of amphetamine (0, 0.3, 0.53, 0.6, 1, 2, 4, 10, 20, 40, 66.7, and 133.3 nM).

**Table S5**. The effect of amphetamine concentration on the Nanozyme assay

| Amphetamine [nM] | Slope a.u×s$^{-1}$ | Slope (nM×s$^{-1}$) | Linearity |
|---|---|---|---|
| 0 | -3.99×10$^{-5}$ | -3.99×10$^{-5}$ | 0.999 |
| 0.3 | -4.00×10$^{-5}$ | -4.00×10$^{-5}$ | 0.999 |
| 0.53 | -4.03×10$^{-5}$ | -4.03×10$^{-5}$ | 0.997 |
| *0.6* | *-4.62×10$^{-5}$* | *-4.62×10$^{-5}$* | *0.999* |
| *1* | *-5.00×10$^{-5}$* | *-5.00×10$^{-5}$* | *0.999* |
| *2* | *-5.40×10$^{-5}$* | *-5.40×10$^{-5}$* | *0.999* |
| *4* | *-5.85×10$^{-5}$* | *-5.85×10$^{-5}$* | *0.999* |
| *10* | *-6.67×10$^{-5}$* | *-6.67×10$^{-5}$* | *0.999* |
| *20* | *-7.99×10$^{-5}$* | *-7.99×10$^{-5}$* | *0.999* |
| *40* | *-9.99×10$^{-5}$* | *-9.99×10$^{-5}$* | *0.999* |
| 66.7 | *-9.99×10$^{-5}$* | *-9.99×10$^{-5}$* | 0.995 |
| 133.3 | -1.00×10$^{-4}$ | -1.00×10$^{-4}$ | 0.984 |

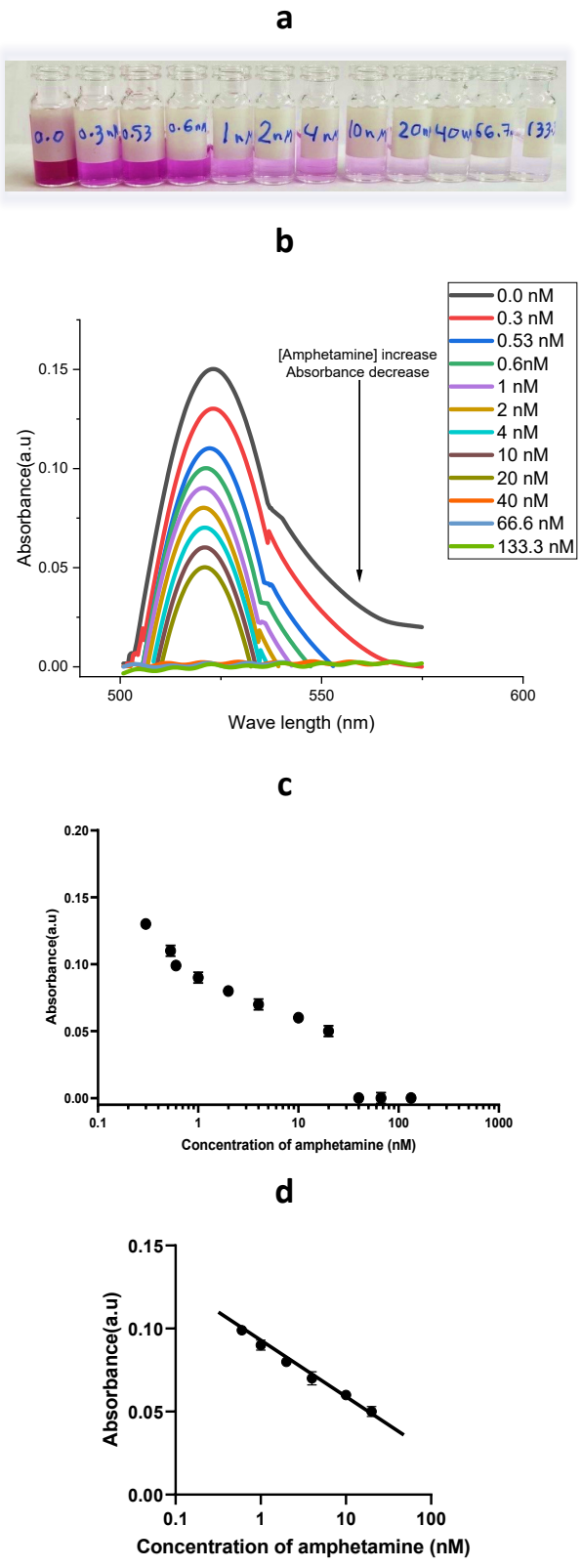


**Figure S9.** Colorimetric assay response for MIP1 at different (a) amphetamine concentration (0.3 to 133 nM) at 1500s. (b) UV-Vis spectra for the assay response at 1500s for different amphetamine concentration (0.3 to 133 nM). (c) Calibration plot of the assay at full amphetamine concentration range and (d) the linear working range (0.6 to 40 nM).

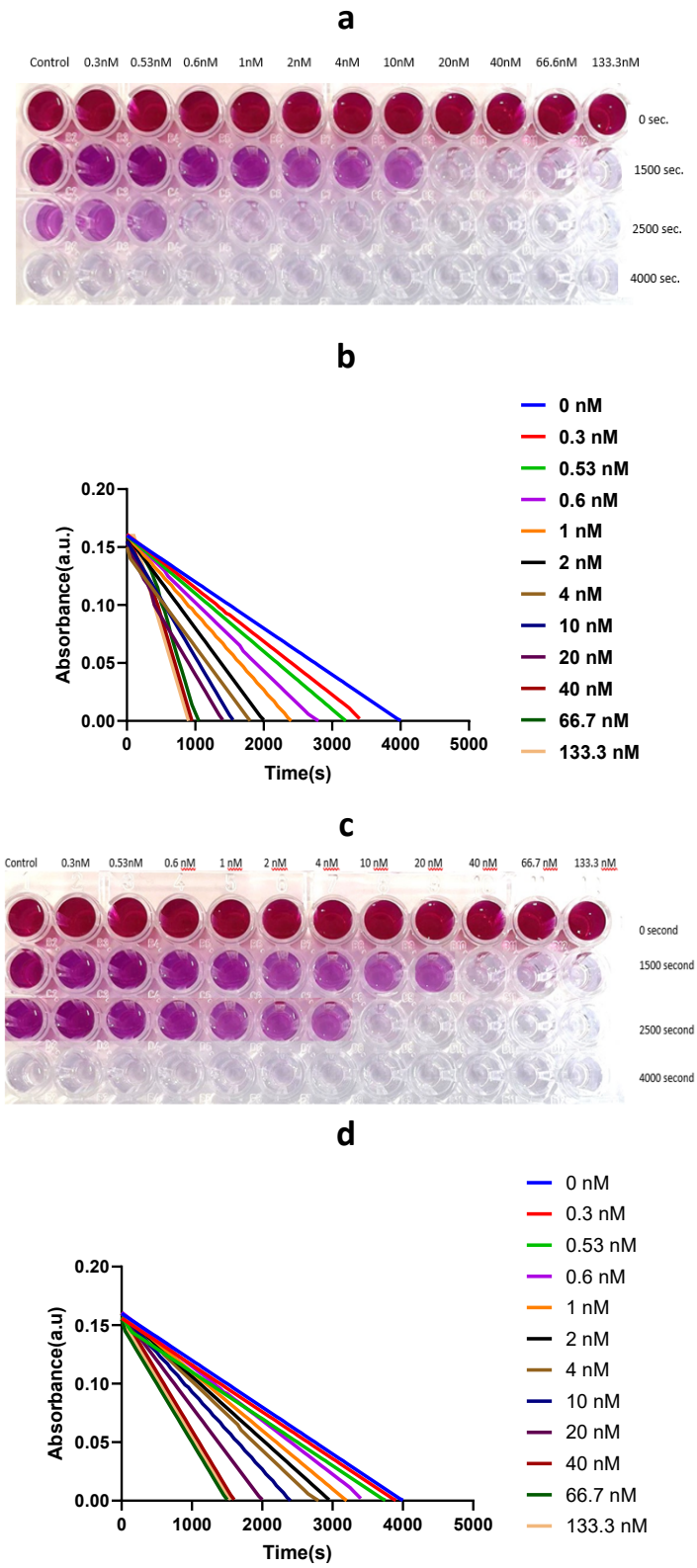


**Figure S10**. Spectroscopic Kinetic measurements for the Nanozyme Colorimetric assay using MIP 1 (a) and (b), and MIP2 (c) and (d), at different amphetamine concentrations (0.3 to 133 nM) and time frames (0 to 4000 seconds). Each well contained 10 µL of the Nanozyme (0.4 mg×mL-1), 135 µL of 10 nM BPR at pH 7 in 5 mM PBS, 135 µL of H2O2 50% and 20 µL of amphetamine.

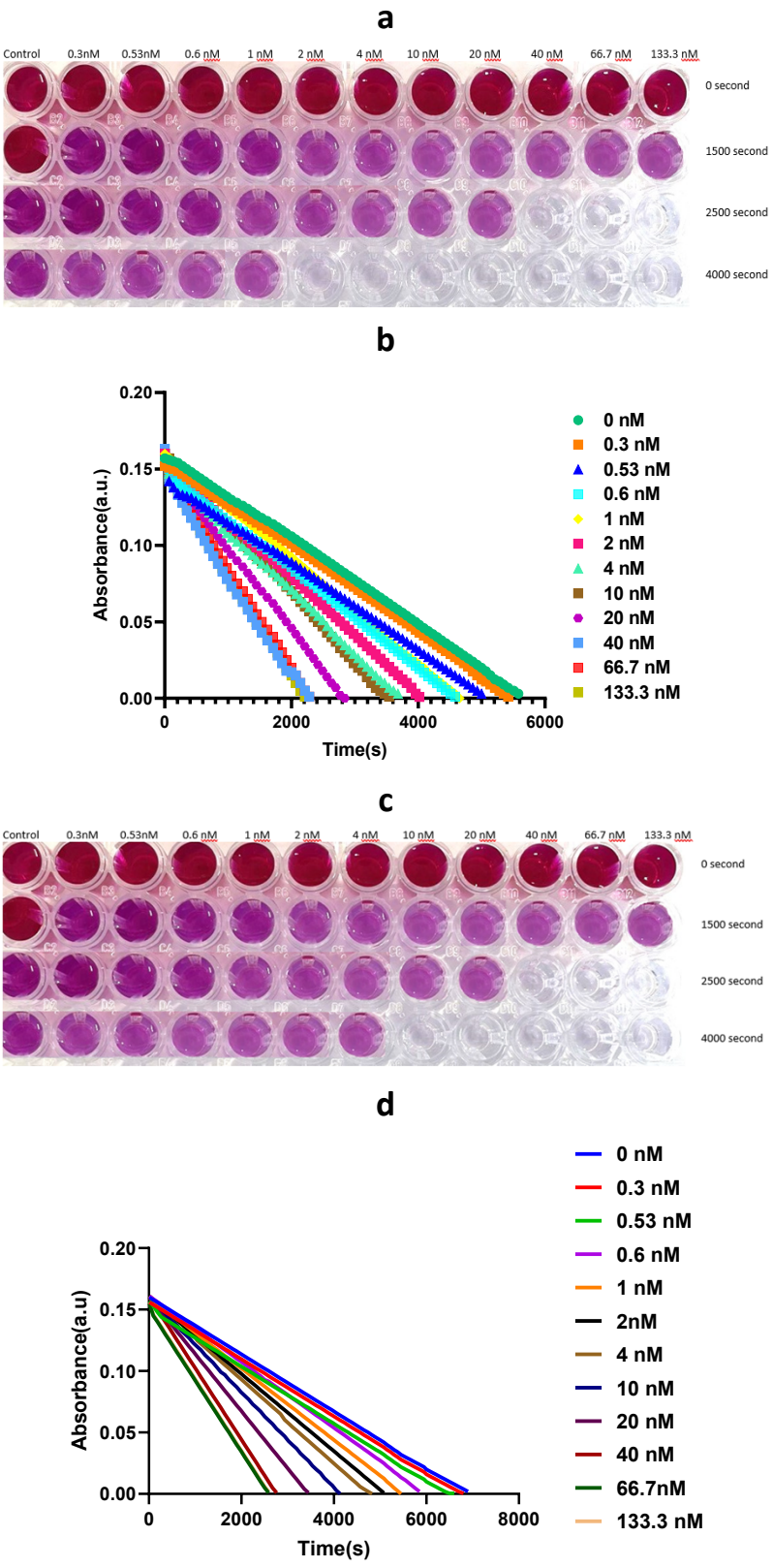


**Figure S11**. Spectroscopic Kinetic measurements for the Nanozyme Colorimetric assay using MIP 3 (a) and (b), and MIP4 (c) and (d), at different amphetamine concentrations (0.3 to 133 nM) and time frames (0 to 4000 seconds). Each well contained 10 µL of the Nanozyme (0.4 mg×mL$^{-1}$), 135 µL of 10 nM BPR at pH 7 in 5 mM PBS, 135 µL of H2O2 50% and 20 µL of amphetamine.

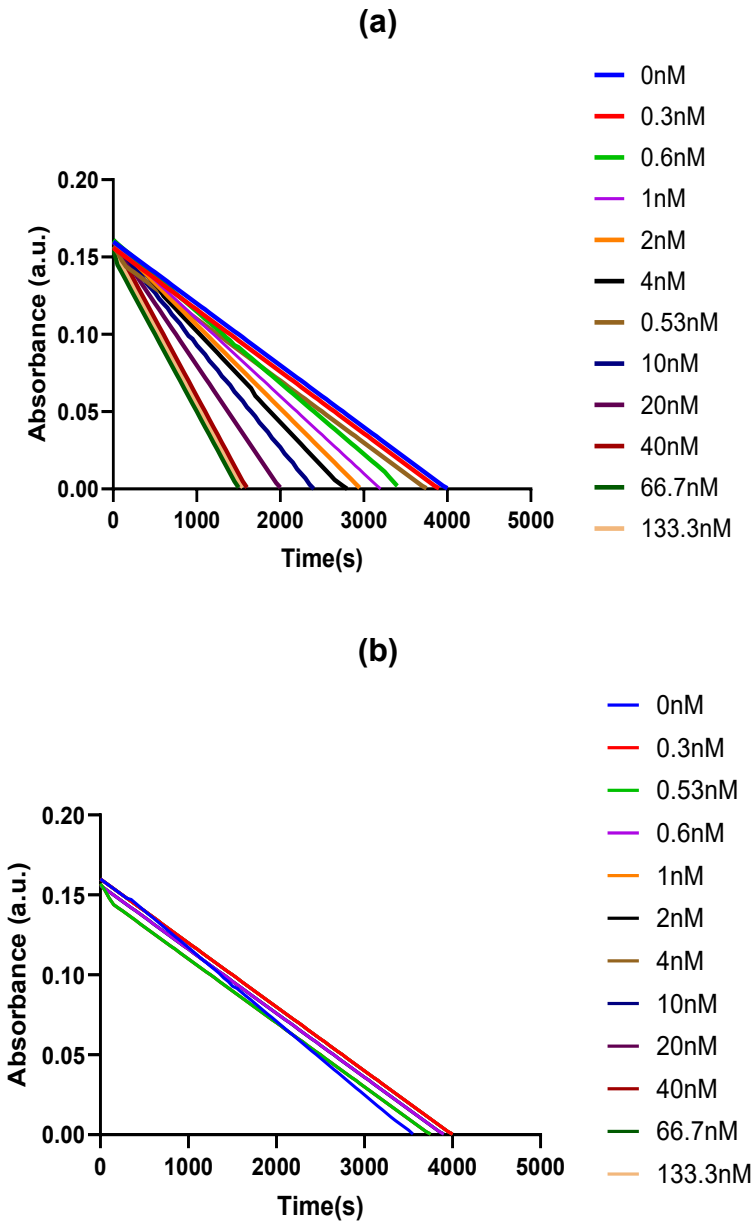


**Figure S12.** Assay comparison between (a) Au/MIP and (b) Au/NIP. Each well contained 10 µL of the Nanozyme (0.4 mg×mL$^{-1}$), 135 µL of 10 nM BPR at pH 7 in 5 mM PBS, 135 µL of $H_2O_2$ 50% and 20 µL of amphetamine (0, 0.3, 0.53, 0.6, 1, 2, 4, 10, 20, 40, 66.7, and 133.3 nM).

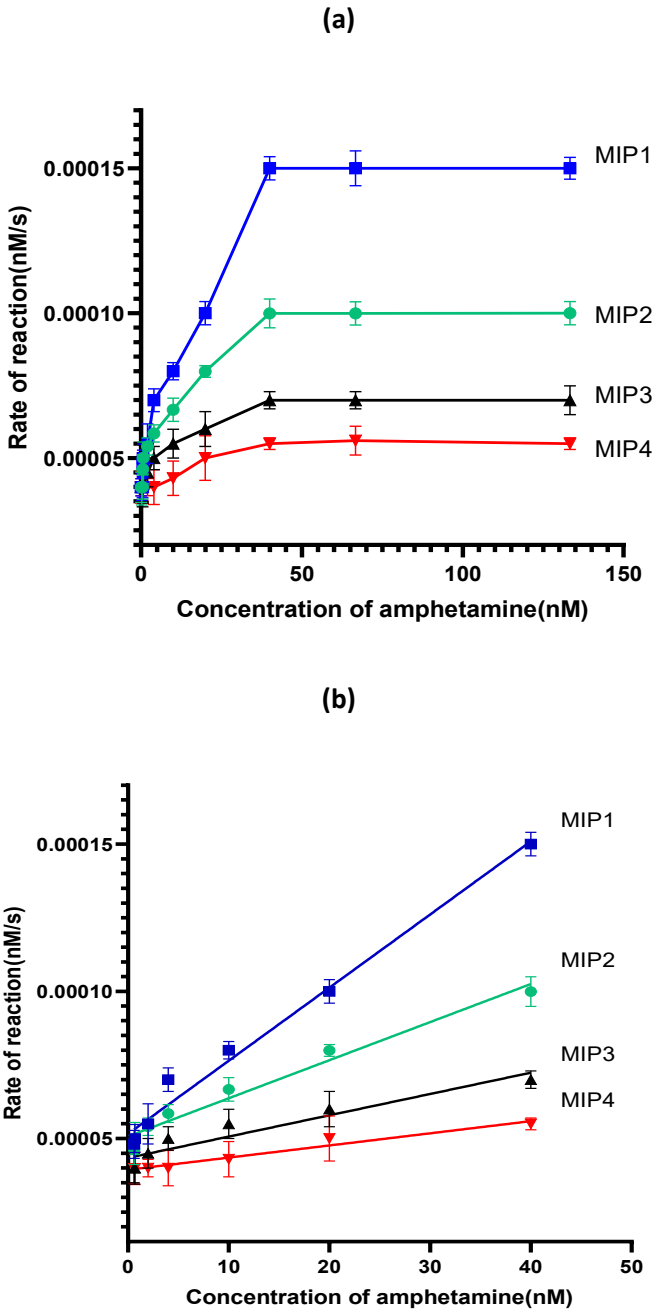


**Figure S13**. Effect of Au/MIP nanozymes with different size of gold core on the assay response to amphetamine. MIP1, MIP2, MIP3, MIP4. Au/MIP nanoparticles prepared varying the size of gold nanoparticles (5,20,50, and 100 nm) with a concentration at 0.06 nM. For the range (a) 0 to 133.3 nM and (b) 0 to 40 nM of Amphetamine. Assay conditions, each well contained 10 µL of the nanozyme (0.4 mg×mL$^{-1}$), 135 µL of 10 nM BPR at pH 7 in 5 mM PBS, 135 µL of $H_2O_2$ 50% and 20 µL of amphetamine.

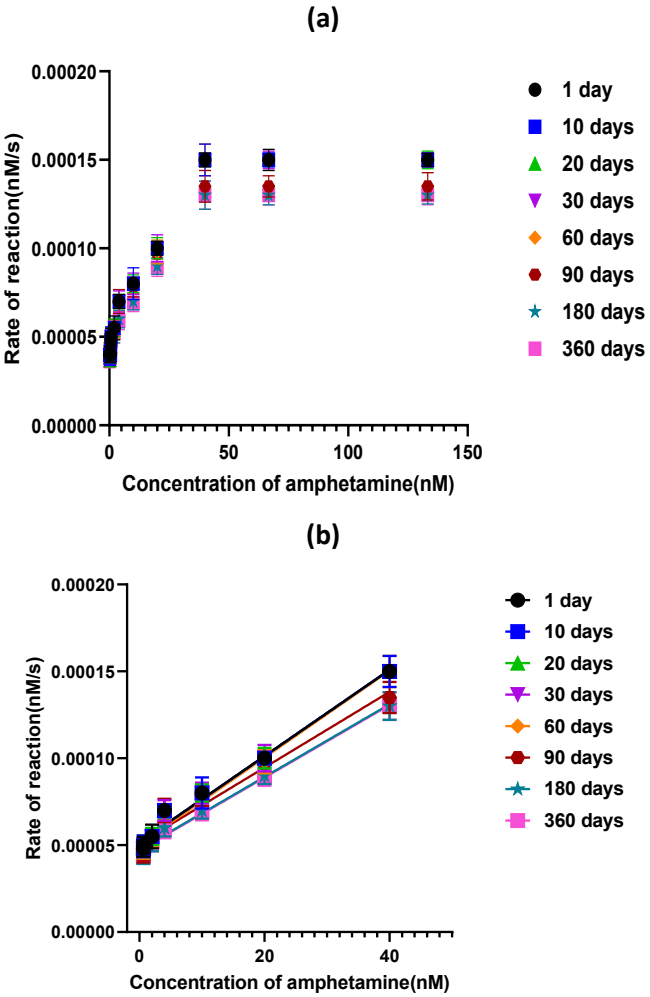


**Figure S14**. Stability of nanozyme assay in different days till 1 year. (a) Assay response and (b)linear range. Nanozyme was stored in solution 4°C in 5 mM PBS.

**References**


1. Ji Y, *et al.* DFT-Calculated IR Spectrum Amide I, II, and III Band Contributions of N-Methylacetamide Fine Components. *ACS Omega* **5**, 8572-8578 (2020).

2. Ismail O, Beyribey B, Turhan K. Removal of Water in Liquid Fuel with a Super Absorbent Copolymer. *Energy Sources, Part A: Recovery, Utilization, and Environmental Effects* **33**, 1669-1677 (2011).

3. Lou-Franco J, Das B, Elliott C, Cao C. Gold nanozymes: from concept to biomedical applications. *Nano-Micro Letters* **13**, 1-36 (2021).

4. Reyhani A, McKenzie TG, Ranji-Burachaloo H, Fu Q, Qiao GG. Fenton-RAFT Polymerization: An "On-Demand" Chain-Growth Method. *Chemistry–A European Journal* **23**, 7221-7226 (2017).

5. Reyhani A, McKenzie TG, Fu Q, Qiao GG. Fenton-chemistry-mediated radical polymerization. *Macromolecular rapid communications* **40**, 1900220 (2019).